# NUMERICAL ANALYSIS OF SOLAR RADIATION EFFECTS AT INDOORS WITH INTERNAL PARTITIONS AND EXTERNAL SOLAR SHADES

**Ali Can Yelekci, Cem Keskin, M. Pınar Mengüç**

Center for Energy, Environment and Economy (CEEE/EÇEM)

& Department of Mechanical Engineering

Ozyegin University, Istanbul, Turkey

**Abstract**

A numerical study is conducted to couple natural convection in an office space with thermal radiation due to solar radiation. The study specifically investigates the effect of partitions located between desks of the office space to develop a tool-box to determine the effect of windows on thermal and visual comfort of occupants. Three different partition cases (according to the aspect ratio of the partition to the ceiling height, which are 0.3, 0.5 and 1.0) were studied. Moreover, the effects of different designs of solar shades in front of windows were investigated. All walls other than the façade of the enclosure are assumed adiabatic, and the enclosure has a single window, which acts as a thermal radiative heat source. All surfaces are assumed to be gray-diffuse surfaces for calculation of thermal radiation. The solar radiation is analyzed for a perfect sunny day with both diffuse and direct sunlight, and for an overcast day with only diffuse sunlight. Based on the choice of partitions geometry, solar shade aspect ratios and the weather conditions, variations on the surface temperature distribution inside the office are analyzed.

*Keywords: Solar radiation, Solar shade, Internal partition, Temperature distribution*

## 1. Introduction

Partitions are used in offices to create personal space for occupants by separating them visually and creating sound insulation. However, if not designed properly, these semi-surrounded cubicles created by the partitions can cause thermal and visual discomfort of internal or external occupants due to unintended effects of thermal radiation and air flow in the office spaces.

There is a large body of literature on the effect of radiation to indoor thermal environment. An analytical and numerical model of radiation configuration factors and solar illumination parameters for a L-shaped room with opaque walls and clear windows was developed (Modest, 1982). Martyushev et al. (2014) numerically studied a cubical enclosure with heat source as a floor, by coupling natural convection and thermal radiation. They concluded that average convective heat transfer (based on dimensionless Nusselt number) is a decreasing, and average radiative Nusselt number is an increasing function of emissivity. Both are increasing function of Rayleigh number (another dimensionless number about the natural convective heat transfer in the medium). Cubical enclosure was numerically studied by Parmananda et al. (2018) with partitions on opposing walls while the other opposing walls were at temperature difference. They obtained that the partitions had little effect on convective Nusselt number but had considerable effect on radiative Nusselt number. Moreover, partitions are observed to cause local temperature differences near them. Xamán et al. (2008) developed a numerical model for a two-dimensional square cavity with a window. They achieved a correlation between the total Nusselt number and the Rayleigh number. The same numerical model was utilized for a study with various window sizes and locations by Olazo-Gómez et al. (2020). They concluded that the radiative heat transfer became lower than the convective heat transfer at higher values of solar irradiance, and the Nusselt numbers for convection and radiation transfer were lower at laminar flow than turbulent flow. Critical review on thermal radiation effects on thermal comfort was presented by Halawa et al. (2014). They emphasized the possible use of mean radiant temperature.

However, there are only a few studies available which explores the effect of thermal radiation coupled with natural convection in an enclosure to explore the thermal comfort of occupants. In addition, a detailed study of, surface


Selection and/or peer review under responsibility of Scientific Committee
doi:10.18086/eurosun.2020.01.03 Available at http://proceedings.ises.org

temperature distribution due to solar thermal radiation within a three-dimensional office environment is missing. Purpose of this study is to shed light on thermal radiation effects of partitions in office spaces to provide better designed offices with better thermal comfort, and to develop more energy efficient spaces. Based on the results obtained, a series of conclusions are listed to achieve these goals.

## 2. Physical and Mathematical Model

The effects of solar thermal radiation on internal partitions in terms of surface temperatures considering thermal radiation is not studied extensively. The geometry for this study is based on an office at our academic building. The research question is investigated by conducting numerical simulations for various aspect ratios and weather conditions (see Tab. 1 for the list of cases). The solar heat flux and solid angle of the radiation incident on the window are assumed to be constant (changing only due to solar shade and weather condition). The diffuse solar irradiance is 10% of the direct solar irradiance. The walls, ceiling and floor are assumed to be adiabatic, except the window and façade, and all the surfaces are analyzed as gray-diffuse surfaces. The air inside of the geometry is assumed to be nonparticipating media. The inlet supplies air at 20° angle from the ceiling to four sides of the inlet cavity.

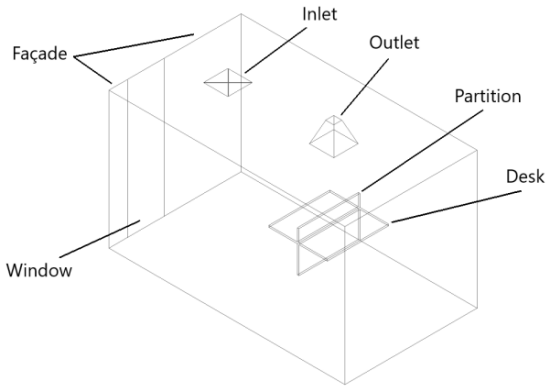


**Fig. 1: Test geometry: An office with desks and partitions; window is allowing solar radiation in**

Since the effect of the solar shade inside the enclosure is the concern of this study, solar shade will be added into the calculations by decreasing both direct and diffuse solar irradiances according to the aspect ratio of the solar shade. Same approach will be applied to the weather condition. For sunny cases both direct and diffuse solar irradiances will be active, but for overcast cases just the diffuse solar irradiance will be active for the model as shown on Tab. 1 for each case.

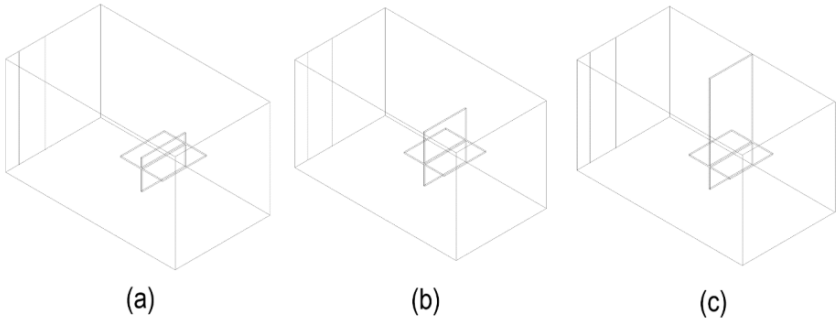


**Fig. 2: Three test geometries for different sizes of partition; partition to ceiling aspect ratios used are (a) 0.30, (b) 0.50 and (c) 1.00**

The material for walls and façade is chosen as concrete, for desk and partition it is wood (see Tab. 2 for material properties). Dimensions of the office are 3.25m x 5.8m x 3.36m. Window is 0.45m away from the side wall. Partition and desk are in the middle of the adjacent wall, both have thickness of 0.04m. Height of the desk is 0.7m. Thickness of the window and façade are 0.015m and 0.15m, respectively.

**Tab. 1: List of cases studied**

| Case Number | Partition Aspect Ratio | Solar Shade Aspect Ratio | Weather Condition | Direct Solar Irradiance [W/m$^2$] | Diffuse Solar Irradiance [W/m$^2$] |
|---|---|---|---|---|---|
| 1a | 0.30 | 0.00 | Sunny | 1366 | 136.6 |
| 1b | 0.50 | 0.00 | Sunny | 1366 | 136.6 |
| 1c | 1.00 | 0.00 | Sunny | 1366 | 136.6 |
| 2a | 0.30 | 0.50 | Sunny | 683 | 68.3 |
| 2b | 0.50 | 0.50 | Sunny | 683 | 68.3 |
| 2c | 1.00 | 0.50 | Sunny | 683 | 68.3 |
| 3a | 0.30 | 0.00 | Overcast | - | 136.6 |
| 3b | 0.50 | 0.00 | Overcast | - | 136.6 |
| 3c | 1.00 | 0.00 | Overcast | - | 136.6 |
| 4a | 0.30 | 0.50 | Overcast | - | 68.3 |
| 4b | 0.50 | 0.50 | Overcast | - | 68.3 |
| 4c | 1.00 | 0.50 | Overcast | - | 68.3 |

**Tab. 2: Material properties**

| Material Name | Density [kg/m$^3$] | $c_p$ [J/kgK] | k [W/mK] | Emissivity | Transmissivity |
|---|---|---|---|---|---|
| Concrete | 2400 | 1000 | 0.8 | 0.94 | - |
| Wood | 800 | 1760 | 0.08 | 0.9 | - |
| Glass | 2500 | 840 | 0.8 | 0.1 | 0.8 |

For all CFD analysis continuity and conservation of mass equations need to be solved. Solution of the energy equation is also required if the problem involves heat transfer. Following Navier-Stokes equations constitute the required equations Çengel et al. (2015). The three dimensional continuity equation is

$$\frac{\partial p}{\partial t}+\frac{\partial (pu)}{\partial x}+\frac{\partial (pv)}{\partial y}+\frac{\partial (pw)}{\partial z}=0 \quad \text{(Eq. 1)}$$

The three dimensional conservation of equations are

$$\frac{\partial (pu)}{\partial t}+\frac{\partial (pu^2)}{\partial x}+\frac{\partial (puv)}{\partial y}+\frac{\partial (puw)}{\partial z}=-\frac{\partial p}{\partial x}+\frac{1}{Re}\left[\frac{\partial \tau_{xx}}{\partial x}+\frac{\partial \tau_{xy}}{\partial y}+\frac{\partial \tau_{xz}}{\partial z}\right] \quad \text{(Eq. 2)}$$

$$\frac{\partial (pv)}{\partial t}+\frac{\partial (puv)}{\partial x}+\frac{\partial (pv^2)}{\partial y}+\frac{\partial (pvw)}{\partial z}=-\frac{\partial p}{\partial y}+\frac{1}{Re}\left[\frac{\partial \tau_{xy}}{\partial x}+\frac{\partial \tau_{yy}}{\partial y}+\frac{\partial \tau_{yz}}{\partial z}\right] \quad \text{(Eq. 3)}$$

$$\frac{\partial (pw)}{\partial t}+\frac{\partial (puw)}{\partial x}+\frac{\partial (pvw)}{\partial y}+\frac{\partial (pw^2)}{\partial z}=-\frac{\partial p}{\partial z}+\frac{1}{Re}\left[\frac{\partial \tau_{xz}}{\partial x}+\frac{\partial \tau_{yz}}{\partial y}+\frac{\partial \tau_{zz}}{\partial z}\right] \quad \text{(Eq. 4)}$$

The energy equation is

$$\frac{\partial (E_T)}{\partial t}+\frac{\partial (uE_T)}{\partial x}+\frac{\partial (vE_T)}{\partial y}+\frac{\partial (wE_T)}{\partial z}=-\frac{\partial (up)}{\partial x}-\frac{\partial (vp)}{\partial y}-\frac{\partial (wp)}{\partial z}-\frac{1}{RePr}\left(\frac{\partial q_x}{\partial x}+\frac{\partial q_y}{\partial y}+\frac{\partial q_z}{\partial z}\right)+\frac{1}{Re}\left[\frac{\partial}{\partial x}\left(u\tau_{xx}+v\tau_{xy}+w\tau_{xz}\right)+\frac{\partial}{\partial y}\left(u\tau_{xy}+v\tau_{yy}+w\tau_{yz}\right)+\frac{\partial}{\partial z}\left(u\tau_{xz}+v\tau_{yz}+w\tau_{zz}\right)\right] \quad \text{(Eq. 5)}$$

Accepted standard value for solar irradiance entering the atmosphere by Howell et al. (2016)

$$I_0 = 1366\ W/m^2 \quad \text{(Eq. 6)}$$

Air mass is used to calculate the solar irradiance incident on the surface of the Earth after losing fraction of the irradiance throughout the atmosphere with corresponding solar zenith angle θ by Roumpakias et al. (2014)

$$AM = \frac{1}{cos\theta} \quad \text{(Eq. 7)}$$

$$I_D = 1.1 \times I_0 \times 0.7^{AM^{0.678}} \quad \text{(Eq. 8)}$$

Equations for the view factors and radiative heat transfer are retreived from Howell et al. (2016). View factor from surface 1 to surface 2 is

$$F_{1-2} = \frac{1}{A_1}\iint_{A_1A_2}\frac{cos\theta_1\theta_2}{\pi S^2}dA_2dA_1 \quad \text{(Eq. 9)}$$

The view factors have reciprocity according to their surface areas

$$A_1F_{1-2} = A_2F_{2-1} \quad \text{(Eq. 10)}$$

Radiative heat transfer inside a grey-diffuse enclosure consists of radiation incident on a surface irradiance, *G*, and radiation leaving the surface radiosity, *J*. Emissivity and absorptivity values are equal, emissivity and reflectivity are equal to 1.

$$\varepsilon_k = \alpha_k \quad \text{(Eq. 11)}$$

$$\varepsilon_k + \rho_k = 1 \quad \text{(Eq. 12)}$$

Radiative heat flux in terms of radiosity and irradiance are shown below

$$Q_k = q_kA_k = (J_k - G_k)A_k \quad \text{(Eq. 13)}$$

$$J_k = \varepsilon_k\sigma T_k^4 + \rho_kG_k = \varepsilon_k\sigma T_k^4 + (1-\alpha_k)G_k = \varepsilon_k\sigma T_k^4 + (1-\varepsilon_k)G_k \quad \text{(Eq. 14)}$$

Calculation of irradiance on a surface inside a grey-diffuse enclosure consists of sum of radiosity values multiplied by the view factors

$$A_kG_k = A_kJ_1F_{k-1} + A_kJ_2F_{k-2} + \cdots + A_kJ_jF_{k-j} + \cdots + A_kJ_kF_{k-k} + \cdots + A_NJ_NF_{k-N} \quad \text{(Eq. 15)}$$

$$G_k = \sum_{j=1}^{N} J_jF_{k-j} \quad \text{(Eq. 16)}$$

Change of temperature of the surface due to solar irradiance involving conduction, convection and radiation is calculated by the following equation. Instead of $q_{solar}cos\theta$ in the equation $I_D$ from the air mass calculation above can be implemented.

$$ka\left(\frac{\partial^2T}{\partial x^2} + \frac{\partial^2T}{\partial y^2} + \frac{\partial^2T}{\partial z^2}\right) + \alpha_sq_{solar}cos\theta + \sigma\varepsilon_i[T_i^4 - T^4(x,y,z)] - \varepsilon_0\sigma T^4(x,y,z) - h(T(x,y,z) - T_e) = mc_p\Delta T/\Delta t \quad \text{(Eq. 17)}$$

Mean radiant temperature is a parameter used for thermal comfort analysis due to radiation by ASHRAE (2009).

$$T_r^4 = T_1^4F_{p-1} + T_2^4F_{p-2} + \cdots + T_N^4F_{p-N} \quad \text{(Eq. 18)}$$

# 3. Numerical Procedure

## 3.1. Validation and Mesh Independence

Validation study for the CFD model was done according to the experimental data obtained by Li et al. (1992) and numerical validation done by Gilani et al. (2016). The experiment was done for an enclosure empty other than a cubical heat. There was a single inlet and an outlet in the enclosure (can be seen on Fig. 3).

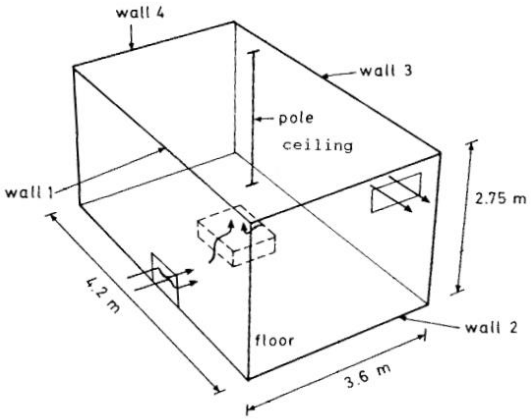


**Fig. 3: Experimental test room geometry by Li et al. (1992)**

B1 case from the experiment was chosen as the validation case by Gilani et al. (2016), due to most amount of result data available on the paper. According to Gilani et al. (2016) B1 case had 300W power output at the cubical heat source, all the walls were painted black, inlet air temperature and speed were 16 °C and 0.102 m/s. Measured ceiling and floor temperatures were 24.5 °C and 24 °C. Calculated heat transfer coefficient on the walls were 10 W/m$^2$-K. Pole (shown on Fig. 3) contained 22 thermocouples during the experiment and validation is done by those thermocouple readings. Fig. 4 indicates the aspect ratio of the point divided by the ceiling height as z/H on y-axis and temperature difference between local temperature and inlet temperature on x-axis validation was done for 0.3 million, 0.7 million and 1.25 million mesh elements. As the number of elements increase results slightly converged towards the experimental data for z/H of 0.1 to 0.4, rest remained unchanged. Due to similarity of the model size similar mesh with the validation case is used on this study, therefore a separate mesh independence analysis was not done for this study as well.

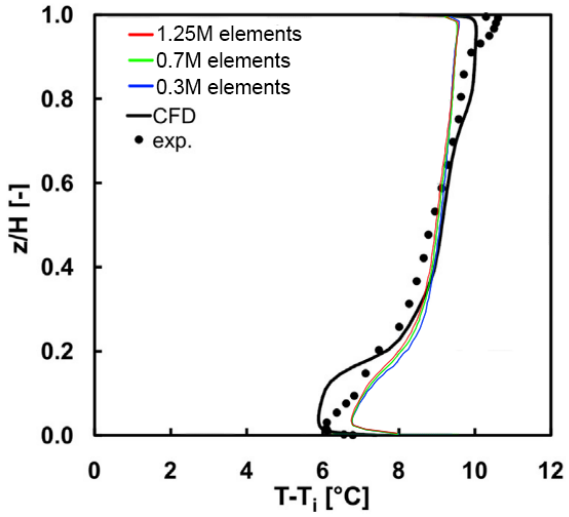


**Fig. 4: Comparison of temperature on the pole between results of experimental (Li et al., 1992), CFD (Gilani et al., 2016) and current study (blue, green and red lines)**

Validation of the CFD was done by ANSYS Fluent 19.2. Turbulence model was chosen as Shear-Stress Transport (SST) k-ω model according to Gilani et al. (2016). Boussinesq approximation was made to simulate the buoyancy effects properly sand air properties are; density is 1.17 kg/m$^3$, specific heat is 1006.95 j/kg-K, thermal conductivity is 0.026 W/m-K, viscosity is 1.83x10$^{-5}$ kg/m-s and thermal expansion coefficient is 0.003 K$^{-1}$. Operating pressure and operating density are 101325 Pa and 1.17 kg/m$^3$. Radiation model was chosen as surface-to-surface (S2S) model. Pressure velocity coupling was chosen as Coupled Algorithm. Pressure discretization was chosen as PRESTO! to best analyze the natural convection due to buoyancy effects. Momentum and energy discretization are second order upwind. Maximum y* value of 1.8 was reached as in the validation study. For convergence criterion; continuity, x-velocity, y-velocity, z-velocity, k and omega were set to 10$^{-3}$, energy and radiation were set to 10$^{-6}$.

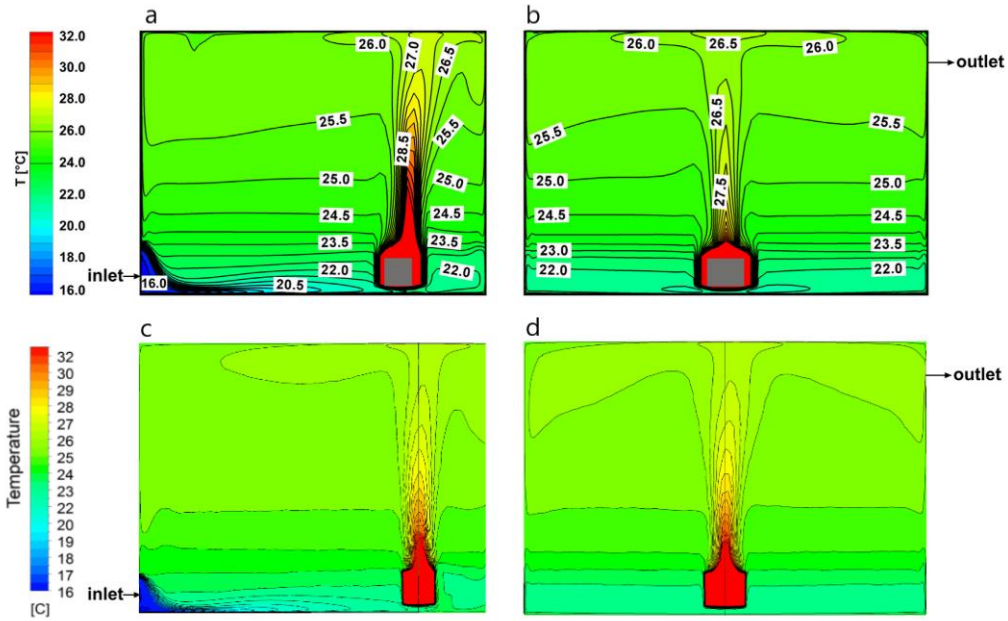


**Fig. 5: Air temperature distribution comparison of Gilani et al. (2016) (a and b) to current study (c and d)**

3.2. CFD Analysis

Physical and mathematical model described above is solved numerically using finite volume method by ANSYS Fluent software. The mesh is constructed from polyhedral elements with inflation on the walls with first layer thickness of 1 mm and total of 15 layers. Desk and partition are modeled as solid all other surfaces are given thickness on the boundary. Conduction heat transfer takes place inside of the desk and partition, through the window and façade. All the surfaces participate in convective and radiative heat transfer. Only façade and window have heat transfer with the environment, all other boundaries are modeled as adiabatic. Zenith angle of the Sun is 45° and the irradiance values are specified for each case above on Tab. 1. View factors were calculated using the ray tracing method with face to face basis and resolution is set to 100. Window is modelled as semi-transparent glass surface. All the models and properties used in this study are identical to the validation study explained at section 3.1. Weather parameters were set to average June weather in Istanbul as 25 °C air temperature and average wind speed of 4.7 m/s. Heat transfer coefficient on the outer surfaces of façade and window are assumed as 23 W/m$^2$K according to the paper by Vincent (2018). Inlet supplies 20 °C air with 1 m/s velocity to four sides of the inlet cavity with a 20° angle from the ceiling. Inlet was modelled according to Sun et al. (2005) without a diffuser to decrease the mesh size significantly. Outlet is modelled as a pressure outlet and has a decreasing cross-sectional area (can be seen on Fig. 1) to prevent reverse flow. Same decreasing outlet model was used at the validation study and it can be seen on Fig. 5 that it does not affect the temperature distribution.

## 4. Results and Discussion

Results are focused on the surface temperatures of desk and partition, since they are the closest surfaces to the occupant and will have the most effect on the occupant's thermal comfort. Desk and partition surfaces are analyzed in two groups for the opposing sides, which are facing the façade and facing the inside of the office. Effect of the partition on the air velocity is shown on Fig. 6 as velocity vectors around the partition and desk. Separation of flow

and increase in vortices due to partition can be observed on theses figures as the partition aspect ratio increases. Also, the air velocity on the desk and partition at the side of the inlet increases with the increasing partition to ceiling aspect ratio. This might create thermal discomfort for the occupant near inlet at higher inlet speeds.

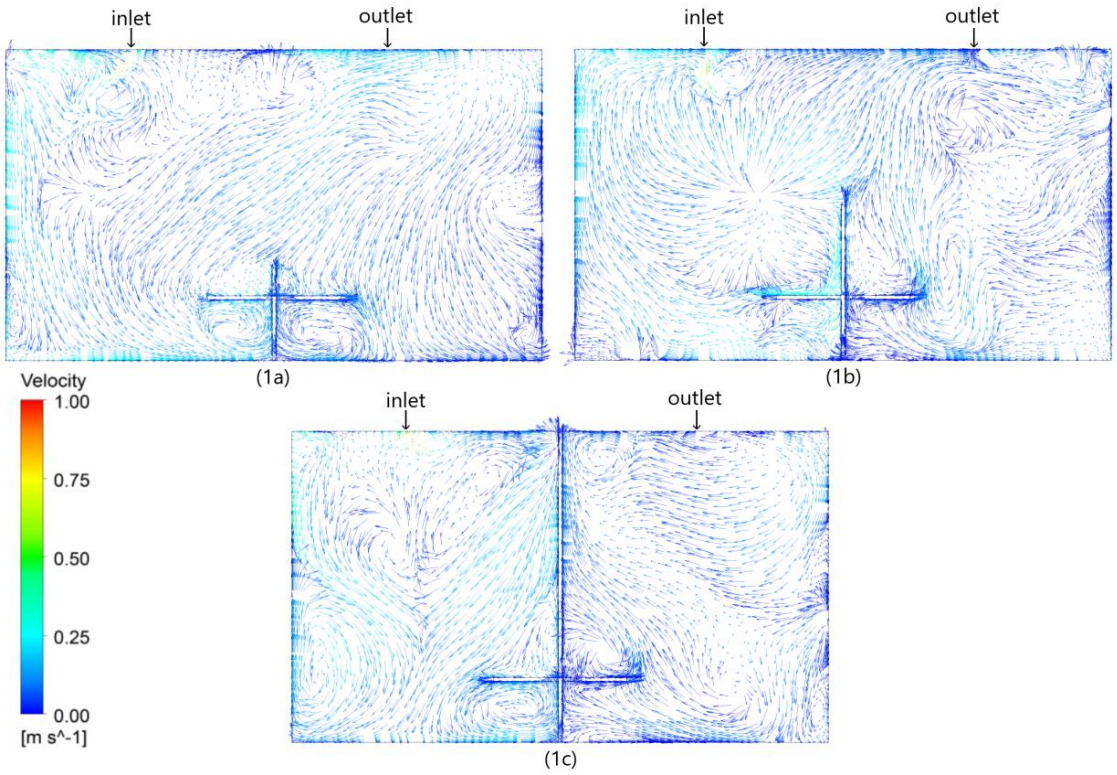


**Fig. 6: Velocity contours on a plane at the middle of the desk (left side is facade)**

Wall temperature contours are shown on Fig. 7 from an isometric viewpoint. Names under each contour represents the case name. On each row of Fig. 7 partition aspect ratio increases from left to right and solar radiation incident on the room decreases from top to the bottom. First row shows the sunny weather cases with no solar shade, second row shows the sunny weather cases with 50% solar shade coverage, third row shows the overcast weather cases with no solar shade and fourth row shows the overcast weather cases with 50% solar shade coverage on the window. As the case names go from 1 to 4 the solar radiation incident on the enclosure decreases. Lack of hot spot on the floor at the third and fourth lines of Fig. 7 is due to lack of direct solar irradiance at overcast weather cases. The colder spot near the top of the window and at the top of the wall between the partition and façade is due to ventilation hitting directly on to those walls.

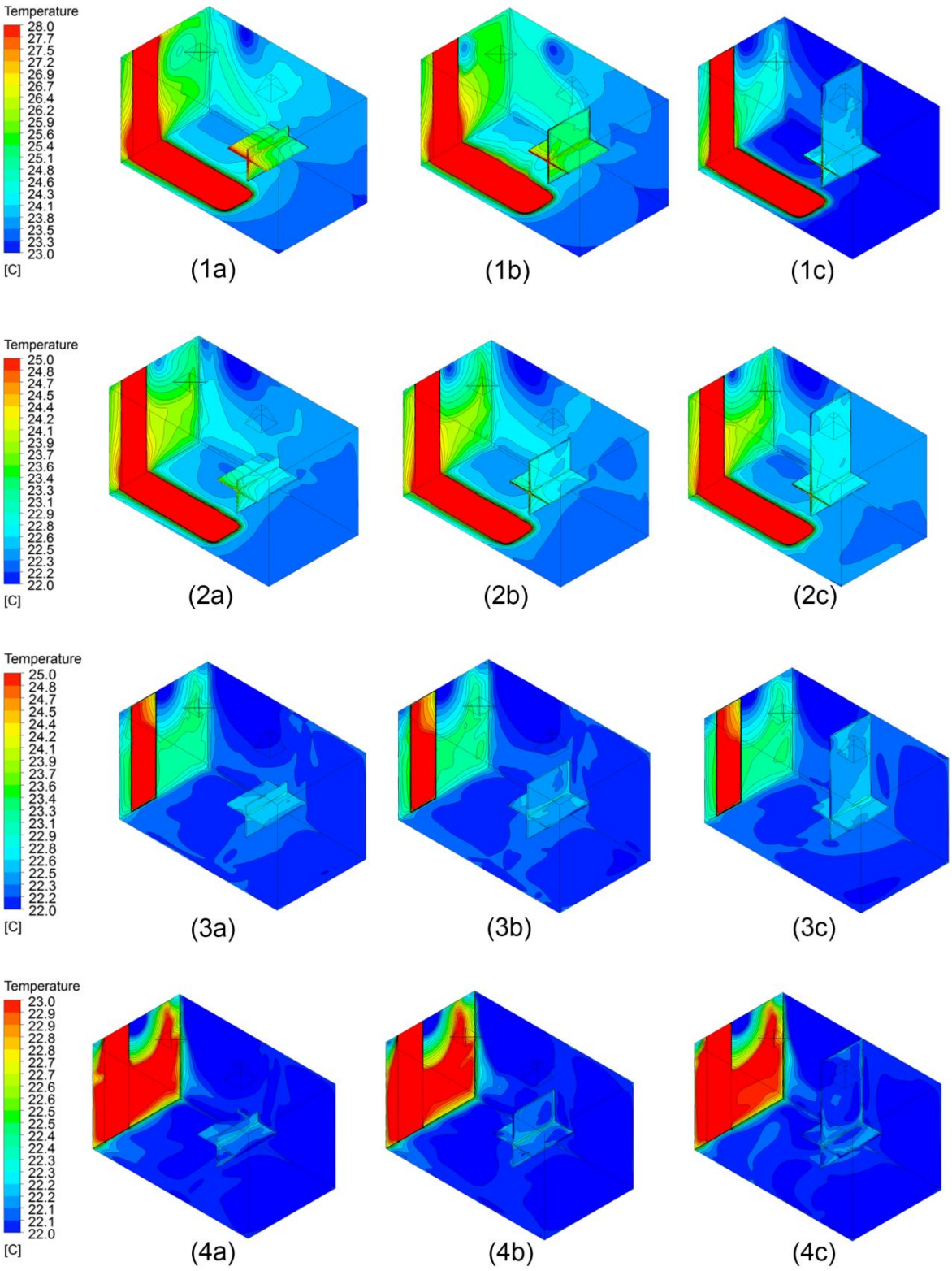


**Fig. 7: Wall surface temperature contours for all cases with a different legend for each corresponding row**

On the contours of Fig. 7 decrease in temperature contrast can be observed as the solar irradiance incident on the enclosure decreases. The effect of partition is minimal for the cases with no direct solar irradiance, since the affect of the partition on surface temperatures can be observed when there is solar radiation present in the enclosure. Surface temperature difference for the opposing sides of the desk and partition makes a peak at 0.5 partition aspect ratio (see Fig. 8). As the partition aspect ratio increases it blocks more solar radiation incident on the back of the enclosure, therefore prevents that region from heating but heats up the side of the desk facing façade even more due to increase

in surface area and viewfactor of the partition. Inlet is located in between the façade and the partition (see Fig. 1) and quarter of the supplied air directly hits the wall between the façade and the desk and the flow separates from the wall to all sides. At partition aspect ratio of 1.0 flow cannot reach the back of the room, because the partition fully blocks the flow (see Fig.6.1c). This prevents the back of the enclosure from cooling down due to ventilation, but causes the region in between partition and façade to cool down more.

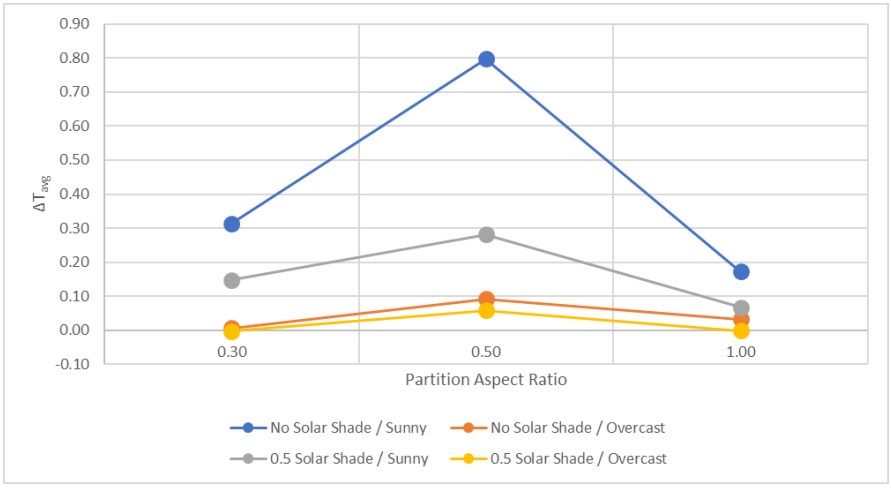


**Fig. 8: Average surface temperature differences ($\Delta T_{avg}$) on opposite sides of the desk and partition (facing façade and facing inside of the office space)**

Average surface temperatures for the opposing sides of the desk and the partition are shown on Fig. 9. Surface temperatures decrease as the solar radiation incident on the enclosure decreases likewise the surface temperature difference between the opposing sides of the desk and partition decrease with decreasing solar radiation.

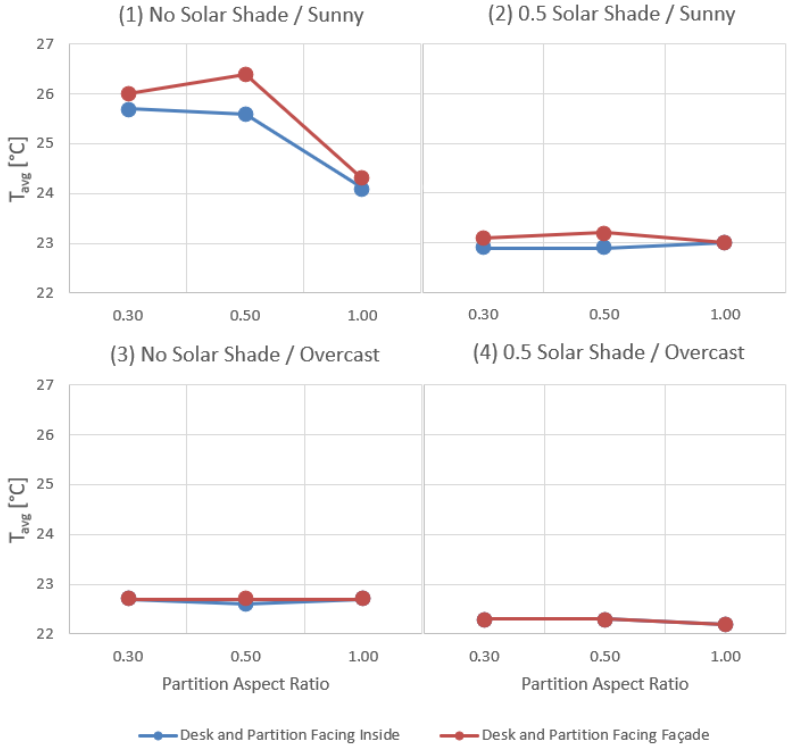


**Fig. 9: Average surface temperatures for opposite sides of desk and partition at different partition aspect ratios**

Average surface temperatures on the Fig. 9 are nondimensionalized on the Fig. 10 for better comparison inbetween cases due to the different temperature ranges at different cases. Nondimensionalization was done by dividing the average surface temperature to the maximum temperature on the desk and partition. Nondimensionalized plots also shows the temperature contrast. At lower the $T_{avg}/T_{max}$ values there is higher temperature contrast (see Fig. 10). The side of the desk and partition facing façade has higher temperature contrast than the side facing inside of the

enclosure. As the solar radiation incident on the enclosure decreases the temperature contrast decreases.

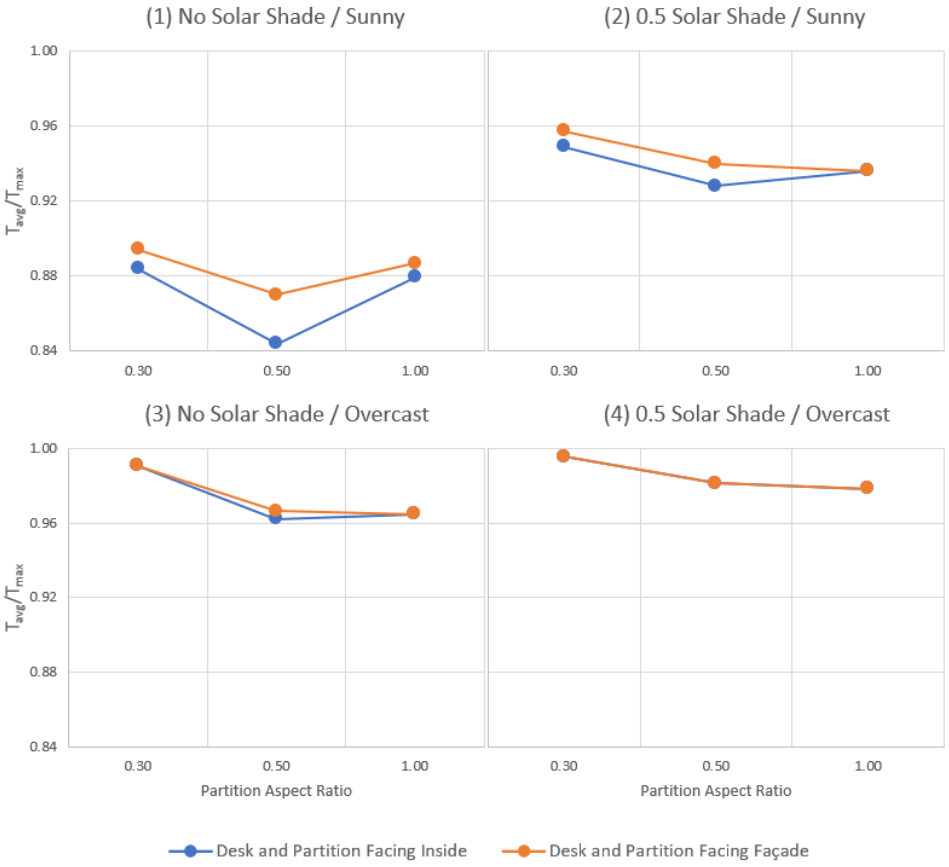


**Fig. 10: Dimensionless average surface temperatures for opposite sides of desk and partition at different partition aspect ratios**

## 5. Conclusion

A numerical study on the effect of indoor partitions has been studied for various external solar shade to window aspect ratios (0.0 and 0.5) and weather condition parameters (sunny and overcast) focused on surface thermal radiation. Surface to surface radiation model which is a gray-diffuse radiation model was utilized for this study. The results were evaluated as surface temperatures and the study focused on the surface temperatures of the desk and partition located at the office, because they are the closest surfaces to the occupants and have highest effect on mean radiant temperatures. Outcomes of the study are:

- Partition creates two zones with different temperature distributions and different air velocities.
- Increasing partition aspect ratio increases the air velocity near the partition and the desk at side facing façade, while decreasing the air velocity at the opposing side.
- Temperature difference at the opposing sides of the partition may cause thermal discomfort for the occupants, due to effected ventilation flow path inside of the office. Increase in air velocity may cause thermal discomfort due to increased convection on the occupant.
- Increasing partition to ceiling aspect ratio increases the temperature difference on the desk and partition for the opposing sides until the partition aspect ratio of 0.5, where the temperature difference peaks, then the temperature difference starts to decrease as the partition aspect ratio reaches 1.0. However, this peak point will alter for different office spaces, partition locations, air supply angles, air supply speeds and inlet locations.
- Partition and desk are the closest surfaces to the occupant, and they have the most effect on mean radiant temperature of the occupant. At higher temperature differences on opposing sides of partition and desk one side of the partition and desk is at higher temperature than the other, which means changing the partition aspect ratio changes the surface temperatures inside the office space and this changes the mean radiant temperature on the occupant causing thermal discomfort.
- Decreasing the solar radiation incident on the enclosure decreases the temperature contrast on the surfaces, therefore the visual comfort increases up until the point where there is enough light present.

## 6. References


- Atlanta, GA, USA: American Society of Heating, Refrigerating and Air-Conditioning Engineers, Inc; 2009 (S.I. Ed.).
- Çengel, Y.A., Ghajar, A.J., 2015. Heat and Mass Transfer Fundementals & Applications, fifth ed. McGraw-Hill Education, New York.
- Gilani, S., Montazeri, H., Blocken, B., 2016. CFD simulation of stratified indoor environment in displacement ventilation. Validation and sensitivity analysis. Building and Environment. 95, 299-313.
- Halawa, E., Hoof, J. V., Soebarto, V., 2014. The impacts of the thermal radiation field on thermal comfort, energy consumption and control—A critical overview. Renewable and Sustainable Energy Reviews. 37, 907-918.
- Howell, J.R., Mengüç, M.P., Siegel, R., 2016. Thermal Radiation Heat Transfer, sixth ed. Taylor & Francis, London.
- Li, Y., Sandberg, M., Fuchs, L., 1995. Vertical Temperature Profiles in Rooms Ventilated by Displacement: Full-Scale Measurement and Nodal Modelling. Indoor Air. 2, 225-243.
- Martyushev, S.G., Sheremet, M.A., 2014. Conjugate natural convection combined with surface thermal radiation in a three-dimensional enclosure with a heat source. International Journal of Heat and Mass Transfer. 73, 340–353.
- Modest, M.F., 1982. A general model for the calculation of daylighting in interior spaces. Energy and Buildings. 5(1), 69–79.
- Olazo-Gómez, Y., Xamán, J., Gijón-Rivera, M., Noh-Pat, F., Simá, E., Chávez, Y., 2020. Mathematical modelling of conjugate laminar and turbulent heat transfer in a cavity: Effect of a vertical glazed wall. International Journal of Thermal Sciences, 152, 106310.
- Parmananda, M., Dalal, A., Natarajan, G., 2018. The influence of partitions on predicting heat transfer due to the combined effects of convection and thermal radiation in cubical enclosures. International Journal of Heat and Mass Transfer. 121, 1179–1200.
- Sun, Y., Smith, T.F., 2005. Air flow characteristics of a room with square cone diffusers. Building and Environment. 40, 589-600.
- Vincent, P.B., 2018. CFD modelling for thermal comfort in an open workspace. eSim 2018, 276-285.
- Xamán, J., Arce, J., Álvarez, G., Chávez, Y., 2008. Laminar and turbulent natural convection combined with surface thermal radiation in a square cavity with a glass wall. International Journal of Thermal Sciences. 47(12), 1630–1638.